

iii. Standard Aperture Dipoles

The arc dipole magnets have a coil i.d. of 80 mm, are 9.7 m long and, with 264 of these magnets required, represent by far the largest single cost item for the collider. In addition, there are 24 insertion dipoles "D8" which are identical to the arc dipoles, and 72 insertion dipoles "D9, D6, D5I and D5O" which are shorter in length.

Dipole Cold Mass

Figure 3-1 shows a cross-section of the dipole cold mass. The dipole design is based on a single-layer "cosine theta" coil, wound from a partially keystoneed, 30-strand NbTi superconducting cable and mechanically supported by a laminated "cold steel" yoke encased in a stainless steel helium containing cylinder. The helium vessel is also a load bearing part of the yoke assembly. This cold mass assembly is mounted within a cryostat consisting of a cylindrical vacuum vessel, an aluminum heat shield, blankets of multilayer thermal insulation, cryogenic headers, and the magnet support system. The nominal dipole operating field is 3.458 T at a current of 5.050 kA and an operating temperature between 4.3 and 4.6 K.

The RHIC dipole cold mass design incorporates a relatively large bore (80 mm), a modest operating field (3.45 T), a single-layer coil, a steel yoke assembled as collars, and no internal trim coils. The general design parameters are listed in Table 3-1.

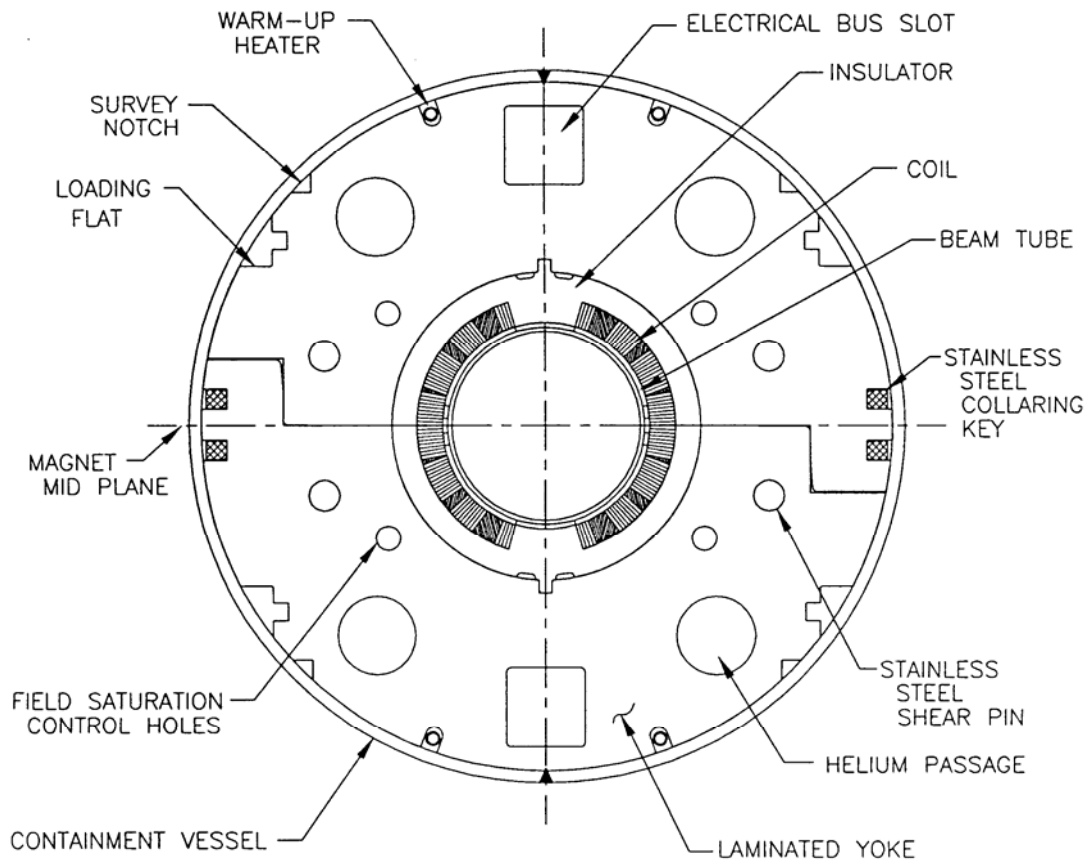


Fig. 3-1. Standard-aperture dipole cold mass cross-section
(coil i.d. = 80 mm).

Table 3-1. Standard Aperture Dipole Parameters

Coil i.d.	(3.15 in.) 80 mm
"ARC" DIPOLES	
No. arc dipoles, two rings	264
No. insertion dipoles, D8	24
Magnetic length, arc and D8	9.45 m
Magnet rigidity - Injection	97.5 T·m
- Top energy	839.5 T·m
Integrated field strength, top energy	32.677 T·m
Dipole field - Injection	0.401 T
- Top energy	3.458 T
Quench field	~ 4.6 T
Operating temperature, max.	4.6 K
Ramp rate, nominal	0.042 T/s
Current - Injection	568 A
- Top Energy	5.093 kA
Lamination length	(379.4 in.) 9.64 m
Cold mass length	(383 in.) 9.73 m
Dipole bending radius, cold	243 m
Mechanical sagitta for 383 in. cold mass length	(1.91 in.) 48.5 mm
Cold mass, including interconnect cans and flange	(7952 lb) 3607 kg
Inductance	28 mH
Stored energy	351 kJ
INSERTION DIPOLES	
No. insertion dipoles, 6.92 m - D5I	12
8.71 m - D5O	12
2.95 m - D6 & D9	48

Table 3-2. Dipole Beam Tube

Outside diameter	(2.875 in.) 73.0 mm
Outside diameter inc. Kapton wrap	(2.883 in.) 73.2 mm
Wall thickness(77 mil)	1.96 mm
Inner diameter, nominal	69 mm
Weight, nominal	(79 lb) 36 kg
Beam tube-coil radial gap	(133 mil) 3.4 mm

Dipole Beam Tube

The dipole utilizes a cold beam tube with dimensions given in Table 3-2. It is centered horizontally inside the coils with 2.7 mm thick by 76 mm long, G-10, longitudinal bumpers with 0.3 m axial spacing and vertically by the RX630 pole pieces, thus defining a helium buffer space. The tube is wrapped with 25 μm Kapton with 60% overlay, providing 76 μm of insulation which is hi-pot tested at 5 kV. The tube is made of seamless, type 316 LN stainless steel, manufactured by Mannesmann Edelstahlrohr, Germany in accordance with the chemical composition requirements of the ASTM A213/A231M specification, but with a nickel content toward the upper part of the allowable range to mitigate potential welding problems at the ends of the tubes. No copper coating on the tube inner surface was required in the RHIC machine. The beam tubes were welded to the end volumes at each end of the magnet, with no intervening bellows.

Dipole Coil

The superconducting coil is assembled from two half-coils that are wound on automated machinery and then formed into a specified size in a precision molding operation. It consists of a single layer of 32 turns per half-coil arranged in four blocks with intervening copper wedges; the size and positions of the wedges and the coil pole spacer have been designed to result in field harmonics meeting the rigid field quality specifications required for RHIC. The four current block design, which has 3 symmetric wedges, is identified as 9B84A in the DRE dipoles. The coil design parameters are given in Table 3-3.

The cable length per half-coil is 1220 m. This cable was insulated with 2 double layers of newly-developed Kapton CI film [AN93a]. The first double layer has polyimide adhesive on the

outer side of the tape; the second has it on both sides. This marked the first use of all-polyimide electrical insulation in the coils of superconducting accelerator magnets, an advance that has greatly improved their electrical integrity. It has also reduced size variations in molded coils, leading directly to improved magnet field quality. The coil ends were designed for relatively simple construction and low harmonic content [KA93a, MO93a]. There are 8 (9) separate spacers in the lead (return) end of each coil, molded of Ultem 6200 plastic. The coils were keyed to the yoke laminations through the precision-molded, glass-filled phenolic (RX630) insulator-spacers. The phenolic insulators separate the coil from the steel yoke and provide both electrical isolation of the coil from ground as well as reduced magnetic saturation effects at high field. The coil design used sufficiently thick midplane caps to allow adjustment of sextupole and decapole harmonics during production [GU94].

Table 3-3. Arc Dipole Coil Design

Inner diameter	(3.146 in.) 79.9 mm
Outer diameter	(3.938 in.) 100.0 mm
Length, overall	(379.75 in.) 9.646 m
Length, coil straight section	(364.80 in.) 9.266 m
Cable length per magnet	(4002 ft) 1220 m
Cable mass per magnet, bare	(220 lb) 100 kg
Effective cable mid-thickness with insulation in.) 1.352 mm under compression	(0.05322
Minimum creep path, conductor to ground	(0.2 in.) 5.1 mm
Dielectric strength:current to ground @ 5 kV	< 200 μ A
Yoke-coil insulating spacer thickness	10 mm
Midplane Kapton thickness	(0.004 in.) 0.10 mm
Cable wrap material thickness, Kapton	(0.001 in.) 25 μ m
Pole angle (coil center radius)	73.178 deg
Number of turns	32
Number of turns, 1st block (closest to pole)	4
Number of turns, 2nd block	8
Number of turns, 3rd block	11
Number of turns, 4th block	9

WEDGE PARAMETERS

<u>Wedge #</u>	<u>Angle</u>	<u>Inner Edge Thickness</u>	<u>Height</u>
1	16.684°	(0.2802 in.) 7.12 mm	(0.382 in.) 9.70 mm
2	9.833°	(0.1217 in.) 3.09 mm	(0.382 in.) 9.70 mm
3	8.105°	(0.0155 in.) 0.39 mm	(0.380 in.) 9.65 mm

Dipole Yoke

The steel yoke performs several functions: it serves as a magnetic return path and thereby enhances the central field, it acts as a “collar” that applies mechanical prestress to the coils through the phenolic insulator-spacer that references the coils to the yoke, and finally, it acts as a shield to reduce stray field in the adjacent ring of magnets. The yoke laminations contain holes for the necessary busses and for the flow of helium. The sizes and positions of these holes, and of the locating notch for the RX630 spacers, were carefully determined to minimize saturation effects [GU94]. Special strain gauge instrumentation and test methods were developed to ensure that the stresses in the magnet met the design goals [GO88a]. Using the yoke laminations as collars dictated the lamination thickness. The magnetic uniformity of the steel was a concern because randomizing of the steel properties through shuffling of laminations was not practicable in a job this large.

The yoke laminations were punched (fine blanked) from 6.35 mm thick ultra-low-carbon steel plate furnished by the Kawasaki Steel Corporation, Japan. Both the mechanical and magnetic characteristics of the steel are important in this application [MO92a]. The yield strength of the steel was specified to be no less than 221 MPa, a level achieved through cold-rolling thickness reduction. This allowed the laminations to be pressed onto the coils without significant yielding on the midplane where the forces during collaring are high. To achieve control of the important high-field saturation magnetization (M_s), the chemical composition (impurities) was strictly specified. This control of the chemistry also ensured that important low field parameters like the coercivity H_c remained under control. Measurements on ring samples [TH92a, MO94a] and chemical analysis of extracted pieces of the production steel were used to monitor the quality of the steel, but the tight quality control exercised by the company in producing the steel ensured that all the material delivered was of the required accelerator quality.

The laminations have an inner diameter of 119.4 mm and an outer diameter of 266.7 mm. They were pinned together in pairs to allow the yoke elements to act as collars. To meet the rms tolerances for the magnetic field integrated over the length of the dipoles, it was required that the weight of steel in the yoke be controlled to within 0.07%. To achieve this tolerance, the lamination pairs that make up the yoke were weighed and their number adjusted to meet the weight specification. The selection of yoke pairs for the top and bottom halves was done in such a way that the total weight of the top half was slightly lower than that for the bottom half [JA95a]. This helped to reduce the skew quadrupole at high fields resulting from a vertically off-centered cold mass in the

cryostat (see Fig. 3-2). During magnet assembly, a press compressed the yoke around the coils. The yoke was subsequently held together with stainless steel keys pushed into notches on the outer circumference. The design preload of 70 MPa acting on the coils was routinely achieved. The yoke laminations extend the full length of the magnet and are not terminated prior to the coil ends as is done in many designs to reduce the field in the mechanically difficult end region of the coils.

Shell

After completion, the coil-in-yoke assembly was surrounded with two, 4.9 mm thick, type 304L stainless steel half-shells, which were then welded along the vertical midplane. The root pass of this weld joined the shell directly to the yoke laminations; no backing strip was used. Extensive testing at Brookhaven confirmed that the joining of these two dissimilar materials gave acceptable results. Nevertheless, a high-nickel-content filler material, type 385LN, was used in this and in the subsequent fill passes to increase the fracture toughness of the joint. In production, these welds were made by automated TIG machines.

Before the welding began, the magnet was placed in a fixture that introduced the required 48.5 mm sagitta; this sagitta was locked in place when the stainless steel half-shells were then welded together. The welding operation also formed the outer, high-pressure (2.1 MPa) helium containment vessel. The shrinkage of the weld compressed the steel collar block, ensuring closure of the mid-plane yoke gap. Further compression was realized at operating temperature from the differential contraction of the stainless steel shell relative to the steel yoke. Compression of the coil increased only until the yoke mid-plane gap closed.

The yoke design parameters are listed in Table 3-4.

Table 3-4. Arc Dipole Yoke and Yoke Containment Design Parameters

YOKE	
Inner diameter	(4.700 in.) 119.4 mm
Outer diameter	(10.5 in.) 266.7 mm
Lamination length	(379.4 in.) 9.64 m
Length, including end plates	(383.0 in.) 9.73 m
Lamination thickness	(0.250 in.) 6.35 mm
Length, lamination packs	(0.500 in.) 12.70 mm
Weight of steel	(6079 lb) 2757 kg
Mechanical sagitta for 383 in. cold mass length	(1.91 in.) 48.5 mm
Bus cavity - width	(1.25 in.) 31.75 mm
- height	(1.25 in.) 31.75 mm
Number of cooling channels	4
Diameter of cooling channels	(1.187 in.) 30.15 mm
YOKE CONTAINMENT SHELL	
Inner diameter, prior to assembly	(10.516 in.) 267.1 mm
Wall thickness	(0.192 in.) 4.9 mm
Weight of shell	(674 lb) 306 kg
ASSEMBLY PRESTRESS	
Room temperature	> (10 kpsi) 68.9 MPa
Cold	> (4.8 kpsi) 33.1 MPa

Table 3-5. Dipole, Electrical Design Requirements

Dipole bus stabilization copper	58 mm ²
Quadrupole bus stabilization copper	58 mm ²
Bus expansion joint motion	46 mm
Warmup heater, resistance/heater @ 300 K	2.24 Ω
Warmup heater, power/heater	938 W
Quench protection diode, max. energy	140 kJ
Quench protection diode, max. reverse leakage current @ 1 kV	10 mA
Quench protection diode, 4.2 K forward voltage threshold @ 10 mA	3.0 V

Electrical Connections and Quench Protection

The design of the machine uses separate main electrical bus systems for the dipoles and the quadrupoles. The bus conductor for these and the various corrector magnets is placed inside an insulating "pultrusion" that is then installed as a completed package into the bus slots at the top and bottom of the yoke. The electrical connections between bus conductors and magnet leads are at the ends of the magnets, within the volume contained by the stainless steel helium containment vessel and end bellows. The end volume also contains the thermal expansion joints for the bus conductors and quench protection diodes. A heater consisting of a stainless steel pipe will accelerate the occasional warm-up of the cold mass.

The quench protection diodes were constructed using a 76.2 mm diameter doped silicon element manufactured by Powerex Corporation, Youngwood, PA. The elements were from an existing compression style hockey puck product line, with the diffusion process modified to achieve the cryogenic requirements. For the RHIC application, a non-hermetic assembly was required. The assembly includes two large copper masses as heat sinks and as compression contacts to the element, and a stainless shell with a threaded top cap. The surface contact with the element is a 76.2 mm circle, loaded to 53.4 kN contact force. The pressure loading is through two 19 mm diameter ceramic balls axially configured to assure an even, concentric loading of the diode element. The top cap is finally welded to the assembly body to prevent thread disengagement during the application of 7000 A test pulses, done at cryogenic temperature. Since the diodes are not hermetic, the polyimide passivation of the junction edge is of paramount importance, and required both visual and electrical

screening to verify passivation integrity. The dipoles were measured to be self-protecting. Quenches of production magnets, mostly near or at the limit of the conductor, had $\int I^2 dt < 12.5$ MIITS, where a MIIT is $10^6 \text{ A}^2 \text{ s}$. Worst-case situations were simulated by using spot heaters to initiate quenches at the midplane of the coil at 5 kA on the last two full-length R&D magnets. (These magnets were nearly identical to the production dipoles.) These spot-heater quenches produced 13.2 and 13.5 MIITS. For these magnets, 11 MIITS corresponded to 300 K, with the temperature determined from voltage taps located near the spot heaters. This measurement was extrapolated to 500 K for 13 MIITS. The threshold temperature for damage was 835 K.

The electrical design parameters for the dipole magnet are listed in Table 3-5.

Dipole Cryostat

The cryostat is the structure which must make the transition from the 4 K environment of the magnet cold mass to ambient temperature as shown in Fig. 1-4. The cryostat must accurately position the magnet cold mass to a given point in the accelerator lattice, while at the same time, minimizing the refrigeration load, by a method that can be implemented reliably in an industrial production setting.

The major components are the carbon steel (ASTM A53) vacuum vessel (outer diameter 610 mm, wall thickness 6.4 mm), the aluminum heat shield (1100-H14) maintained at a nominal temperature of 55 K, blankets of multilayer aluminized Mylar thermal insulation, various cryogenic headers including bellows at their ends, and post-type supports [SO91a] that carry the cold mass weight to the wall of the vacuum tank. Each support post is comprised of two identical molded plastic "hats" attached end to end. They were precision molded as tubes with flanges from Ultem 2100 glass-filled plastic. A standard arc dipole has three such supports. They make sliding contact (where necessary) to the cold mass to support the cold mass inside the cryostat. A spring was incorporated into this contact assembly to maintain the horizontal alignment of the cold mass. In the tunnel, only two stands carry the load to the ground. The weight distribution is 40 % on the center post and 30 % on each of the outer posts. The post inner diameter is 212.8 mm with a wall thickness of 4.8 mm. The heat shield is captured between the top and bottom hats. The heat leak per leg is 0.1 W to 4.5 K and 1.0 W to 55 K. The superinsulation blankets use alternating layers of reflectors (6 μm non-crinkled Mylar, aluminized on two sides) and spacers (0.15 mm REEMAY 2006). In order to minimize the heat load, the thickness of the aluminum on the Mylar used at 4.5 K is thicker (600 \AA) than that on the Mylar at 55 K (380 \AA) because of the difference in wavelength of the shielded radiation. The legs of the vacuum chamber are carbon steel castings welded to the vacuum vessel. Sockets machined into these legs are used to provide the exterior survey fiducial references; survey fixtures translate the positional information provided by the cold mass to these references.

The cryostat design parameters are given in Table 3-6.

Table 3-6. Dipole Cryostat

Vacuum vessel, o.d.	(24 in.) 610 mm
Vacuum tank, wall thickness	(0.25 in.) 6.4 mm
Heat shield, o.d.	(21.0 in.) 533 mm
Heat shield, wall thickness, upper section	(0.09 in.) 2.3 mm
Heat shield, wall thickness, lower section	(0.125 in.) 3.2 mm
Recooler supply header, i.d.	(2.71 in.) 68.8 mm
Helium return header, i.d.	(2.71 in.) 68.8 mm
Utility header, i.d.	(2.71 in.) 68.8 mm
Shield cooling pipe, i.d.	(2.157 in.) 54.8 mm
Number supports	3
Support spacing	(141.5 in.) 3.59 m
Weight distribution	
Center post	40%
	(3395 lb) 1540 kg
Outer post ea.	30%
	(2532 lb) 1148 kg
Post, i.d.	(8.38 in.) 212.8 mm
Post, wall thickness	(0.189 in.) 4.8 mm
Heat leak per leg at 4.5 K	0.1 W
Heat leak per leg at 55 K	1.0 W
Superinsulation layers, cold mass only	17 Reflector, 32 Spacer
Superinsulation layers, cold mass plus piping	38 Reflector, 53 Spacer
Superinsulation layers, shield	62 Reflector, 62 Spacer

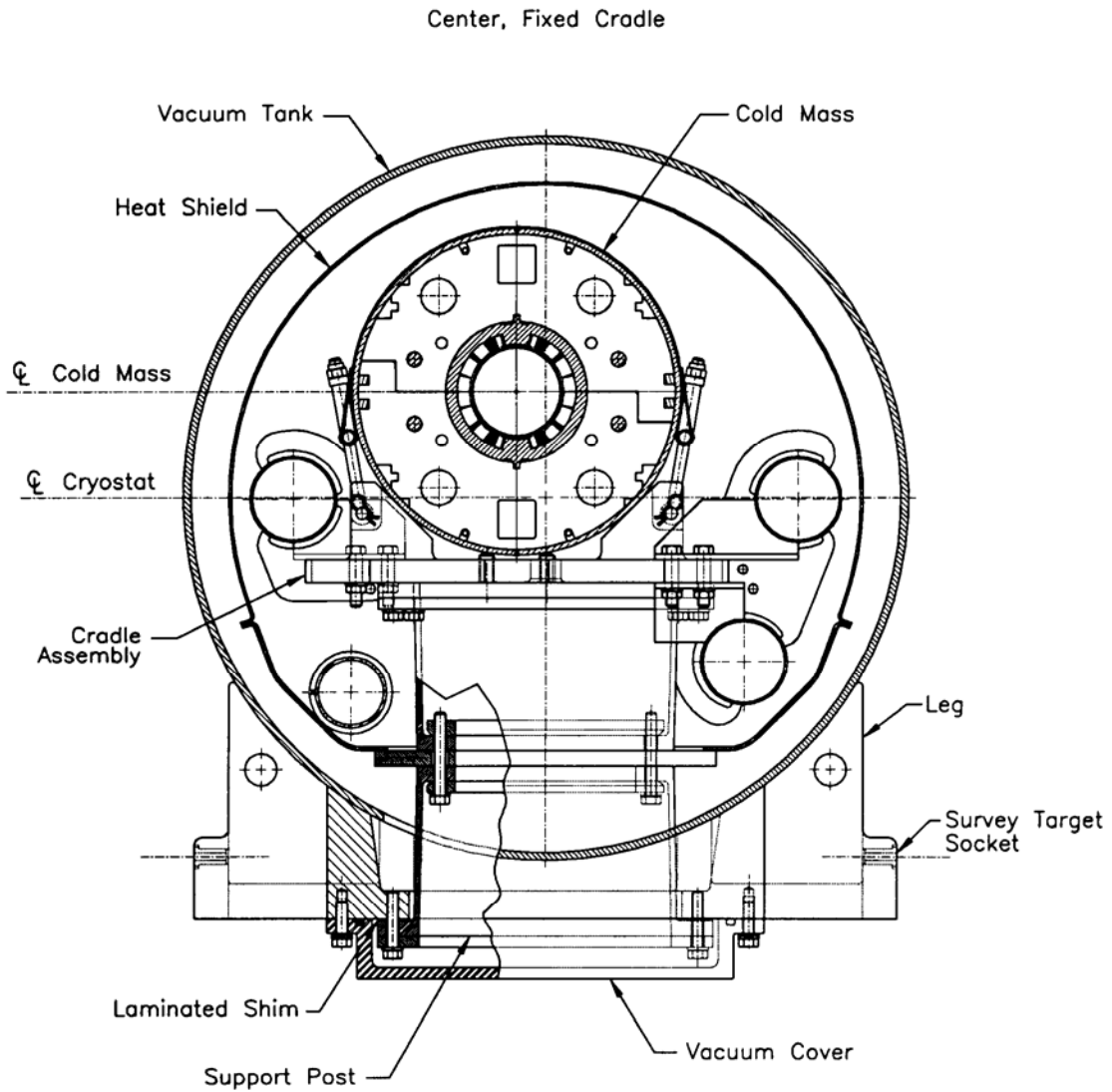


Fig. 3-2. Arc dipole cross-section (610 mm vacuum vessel o.d.).

Magnet Manufacture, Delivery and Acceptance

A total of 373 dipole magnets was manufactured at Grumman according to prints and specifications developed by Brookhaven [WA95b, AN95a, FI99a]. They were delivered as complete units ready for installation into the RHIC lattice. Superconducting cable, beam tubes and quench protection diodes were supplied by Brookhaven; all other components were procured by Grumman. During their construction, the magnets were subjected to rigorous quality and performance checks designed to prevent the manufacture of any faulty magnets. This goal was achieved; all magnets delivered to Brookhaven were acceptable for machine use. The initial 30 magnets were cold tested at Brookhaven. Upon confirmation that their performance validated their design and manufacture, only about 10% of the remaining magnets were cold tested. This reduced level of testing, and the resultant significant cost savings, has been proven sound by the subsequent stellar magnet performance in the machine. Warm magnetic measurements were made on all magnets, both at Grumman [GU95a] and at Brookhaven, and the good warm-cold correlation has been used in tracking calculations at Brookhaven to predict machine performance.

Performance

Quench test results for the 51 arc dipoles tested at 4.5 K are shown in Fig. 3-3. The magnets were quenched until a “plateau,” where there was little variation in quench current, was reached, typically within a few quenches. The quench performance of the magnets was excellent. The initial quench current and the plateau quench current of each magnet exceeded the 5 kA operating current. The plateau quench currents were consistent with the currents expected for magnets operating at the current-carrying limit of the superconductor. In RHIC operations, the rings have reached 5 kA without quenching the arc dipoles, confirming the good construction of these magnets.

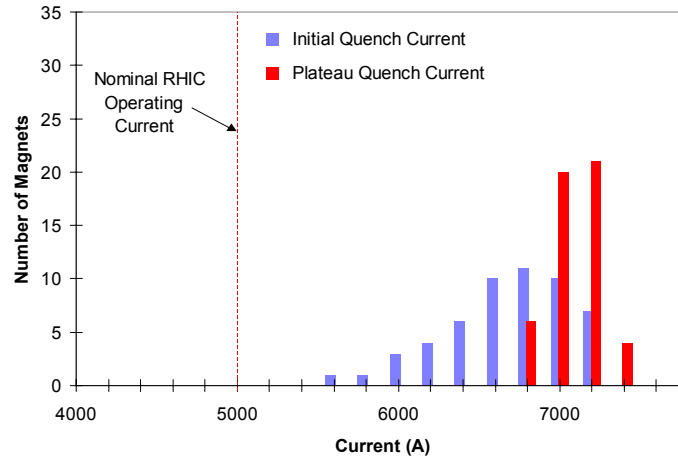


Fig. 3-3. Quench performance of 51 arc dipoles, tested at 4.5 K. The average plateau quench current of these 51 magnets was 7101 A; the field at this average quench current is 4.52 T.

Magnetic measurements were made with two probes: a 1 m-long rotating coil with attached gravity sensor and a 10 m-long stationary coil. The 1 m coil was used to measure the harmonics and the field angle. Integral values of the harmonics and field angles at 4.5 K were obtained by moving the coil in ten 1 m steps at three currents: near the planned injection current (660 A), at transition in RHIC (1450 A), and at full energy (5 kA). Measurements were also made at closely spaced current steps with the coil at a fixed axial position near the center of each magnet. The 10 m stationary coil was used to measure the integral dipole field. The 1 m and the 10 m coils were also used for “warm” measurements with the magnets at room temperature.

During production, several changes were made to the magnet cross section and, thus, to the geometric harmonics [WA98]. Planned changes were introduced in order to reduce the harmonics. Some unplanned changes in transfer function occurred due to variations in the materials used in the magnets. These changes were corrected before too many magnets were affected. The impact of affected magnets on RHIC was reduced by carefully assigning magnets with lower than normal transfer function to lattice locations next to magnets with higher than normal transfer function [WE95].

The field quality of the magnets at room temperature (“warm”) was well correlated with the field quality at 5 kA (“cold”). Integral measurements of the low-order harmonics (normal and skew quadrupole, normal sextupole, and normal decapole) are shown in Figs. 3-4 through 3-7. (The data do not lie on the straight line in the plots because of effects such as saturation.) Measurements of

these same four harmonics as a function of current, in the straight section of the magnets, are shown in Figs. 3-8 through 3-11, along with the calculated values. Warm and cold measurements of the harmonics through the 22-pole term are given in Table 3-7. (Note that the quadrupole term is denoted by $n = 1$. Harmonics are expressed in “units”, where a unit is 10^{-4} of the main field.)

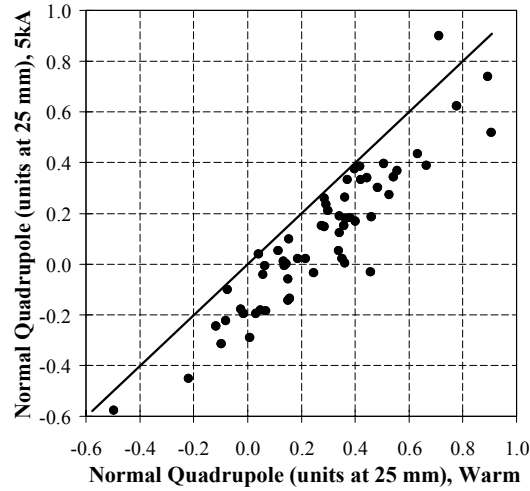


Fig. 3-4. Measured warm-cold normal quadrupole correlation.

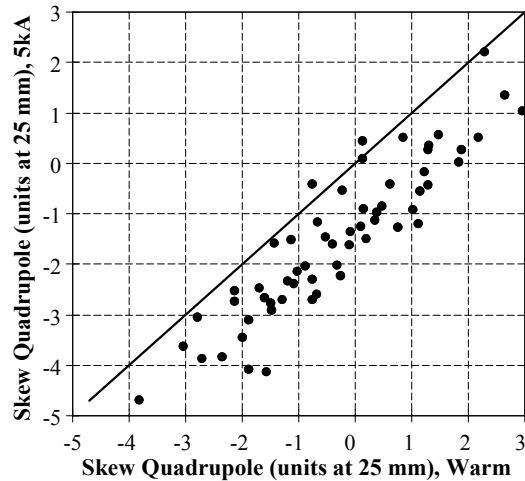


Fig. 3-5. Measured warm-cold skew quadrupole correlation.

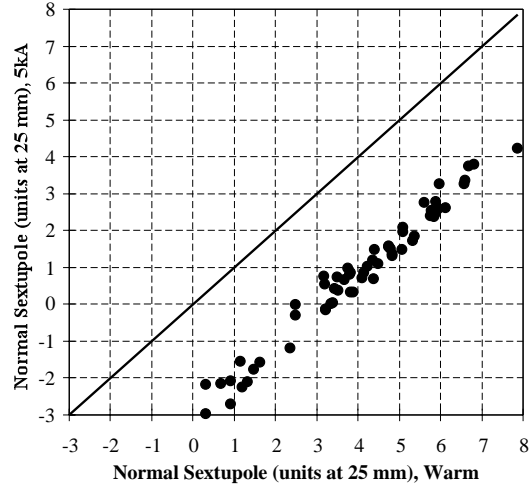


Fig. 3-6. Measured warm-cold sextupole correlation.

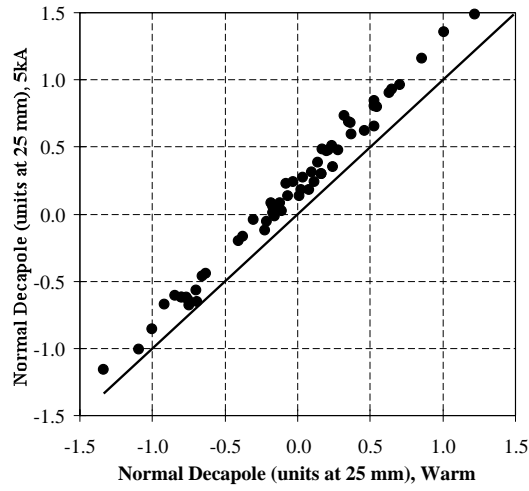


Fig. 3-7. Measured warm-cold decapole correlation.

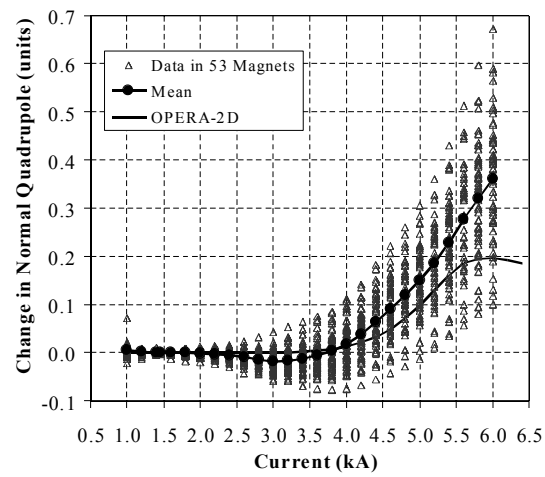


Fig. 3-8. Current dependence of the normal quadrupole component in the 80 mm dipole.

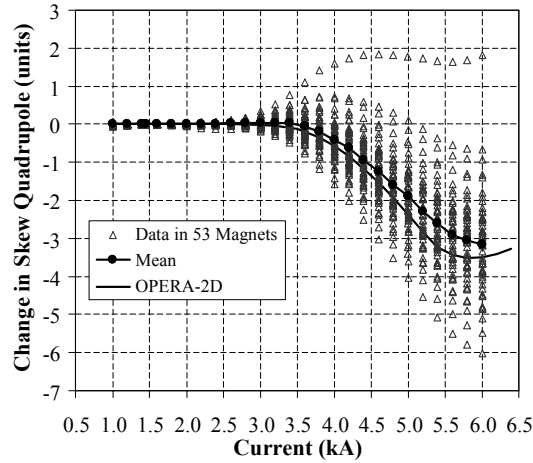


Fig. 3-9. Current dependence of the skew quadrupole component.

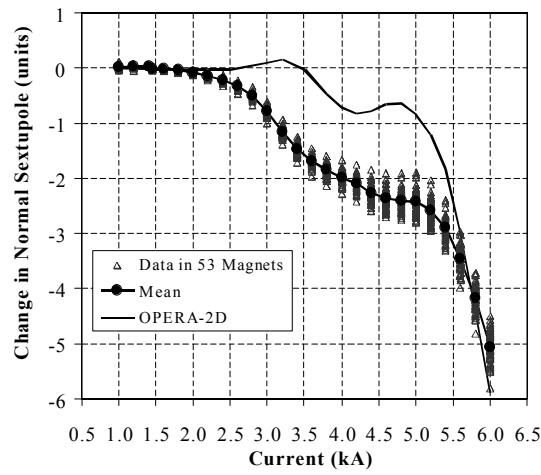


Fig. 3-10. Current dependence of the normal sextupole component.

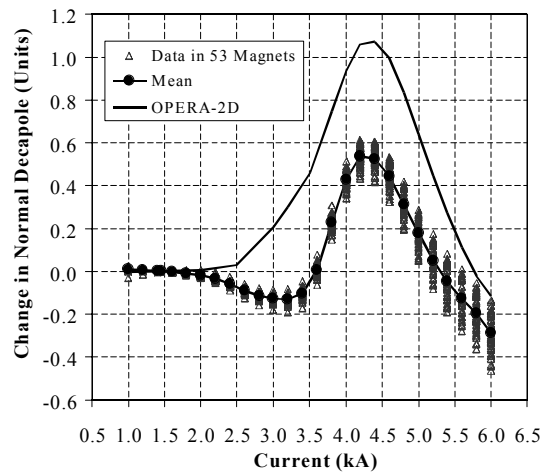


Fig. 3-11 Current dependence of the normal decapole component.

Table 3-7. Summary of the measured integral field harmonics in the 80 mm aperture, 9.7 m long dipoles. The 30 A measurements were done while the magnet was at room temperature. Harmonic b_1 is the normal quadrupole term.

Harmonic	Mean			Standard Deviation		
	30 A (296 magnets)	660 A (58 magnets)	5000 A (59 magnets)	30 A (296 magnets)	660 A (58 magnets)	5000 A (59 magnets)
b_1	0.25	0.08	0.10	0.37	0.28	0.28
b_2	3.54	-0.17	0.83	1.74	2.22	1.76
b_3	-0.03	0.00	0.01	0.10	0.08	0.08
b_4	0.22	-0.33	0.15	0.44	0.57	0.59
b_5	0.01	0.00	-0.03	0.03	0.03	0.04
b_6	0.12	-0.13	1.19	0.11	0.13	0.14
b_7	0.00	-0.01	-0.01	0.01	0.01	0.01
b_8	0.09	0.14	0.12	0.11	0.12	0.12
b_9	0.00	0.02	0.02	0.01	0.02	0.02
b_{10}	-0.53	-0.58	-0.58	0.02	0.02	0.02
a_1	-0.20	0.28	-1.51	1.62	1.53	1.51
a_2	-1.11	-1.03	-1.07	0.20	0.17	0.18
a_3	-0.01	-0.03	-0.36	0.49	0.42	0.41
a_4	0.18	0.21	0.20	0.07	0.06	0.06
a_5	-0.01	0.02	-0.06	0.17	0.15	0.16
a_6	-0.11	-0.10	-0.10	0.03	0.02	0.02
a_7	0.00	-0.01	-0.01	0.05	0.05	0.05
a_8	0.02	0.02	0.02	0.01	0.01	0.01
a_9	0.00	0.04	0.04	0.01	0.02	0.02
a_{10}	-0.01	-0.01	-0.01	0.00	0.01	0.01

The rms variation of the integral transfer function B/I measured warm in all the 9.7 m dipoles was 3.2×10^{-4} . The distribution of the ratio between the integral transfer functions measured warm and at 1.45 kA had an rms of 1.8×10^{-4} . A measurement of the transfer function in the straight section of the magnet whose transfer function is closest to the mean is shown in Fig. 3-12. The mean systematic twist of the dipoles was 0.6 mrad, with a rms of 2.2 mrad.

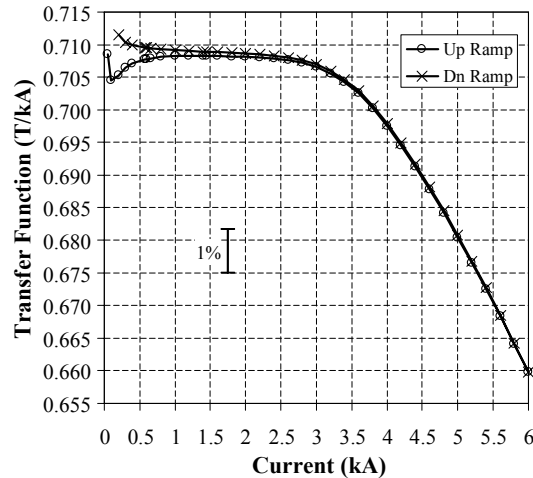


Fig. 3-12. Transfer function for a typical 80 mm dipole in the straight section.

The time dependence of the 80 mm dipoles was determined from measurements in one of the 2.95 m-long magnets built for the D6 and D9 positions (see Table 1-1). The measurements were focussed on the time dependence during injection and at the start of the ramp up [JA00]. The 1 m tangential measuring coil was located in the straight section of the magnet. Measurements were made with a time resolution of ~ 0.66 sec. A smooth current ramp with a quadratic dependence of current on time was used. Prior to the measurement, the magnet was cycled from 25 A to 5.1 kA and back to 25 A at 60 A/sec. The magnet was then ramped to 470 A at 40 A/sec, held at that current, and then ramped up at 40 A/sec. The time variation of the transfer function and the current for injection and the initial part of the ramp up are shown in Fig. 3-13. The change of the transfer function at injection current and the “snapback” at the start of the ramp can be seen in the data. The drift and snapback of the sextupole were ~ 1.5 units. The snapback to the initial value occurs when the current has increased from 470 A to ~ 498 A. The snapback is faster at higher ramp rates (~ 5 -6 sec at 20 A/sec, ~ 2 sec at 70 A/sec.). Because the superconductor was purchased as a single lot, it was expected that magnets of the same type would behave in a similar way. This was confirmed by measurements made on the RHIC beam [FI00].

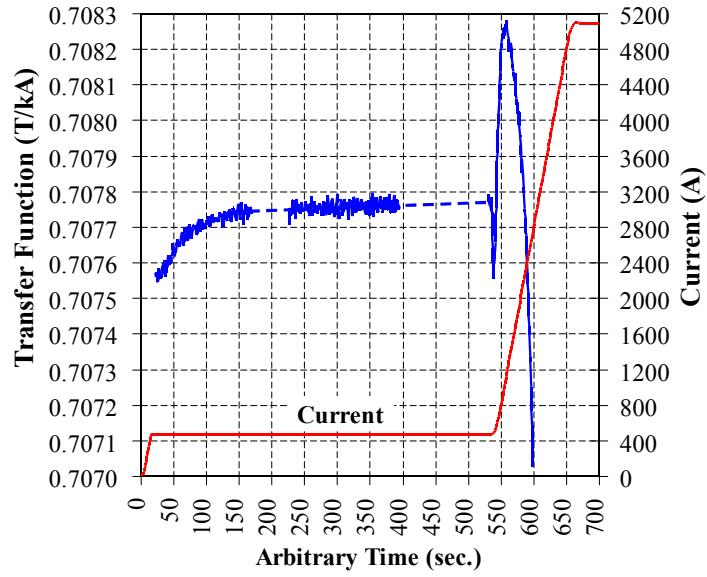


Fig. 3-13. Time decay and snapback in D96525.